

Bioactive Glass Stimulates In Vitro Osteoblast Differentiation and Creates a Favorable Template for Bone Tissue Formation

C. LOTY,^{1,2} J.M. SAUTIER,¹ M.T. TAN,³ M. OBOEUF,¹ E. JALLOT,⁴ H. BOULEKBACHE,⁵
D. GREENSPAN,³ and N. FOREST¹

ABSTRACT

In this study, we have investigated the behavior of fetal rat osteoblasts cultured on bioactive glasses with 55 wt% silica content (55S) and on a bioinert glass (60S) used either in the form of granules or in the form of disks. In the presence of Bioglass granules (55 wt% silica content), phase contrast microscopy permitted step-by-step visualization of the formation of bone nodules in contact with the particles. Ultrastructural observations of undecalcified sections revealed the presence of an electron-dense layer composed of needle-shaped crystals at the periphery of the material that seemed to act as a nucleating surface for biological crystals. Furthermore, energy dispersive X-ray (EDX) analysis and electron diffraction patterns showed that this interface contains calcium (Ca) and phosphorus (P) and was highly crystalline. When rat bone cells were cultured on 55S disks, scanning electron microscopic (SEM) observations revealed that cells attached, spread to all substrata, and formed multilayered nodular structures by day 10 in culture. Furthermore, cytoenzymatic localization of alkaline phosphatase (ALP) and immunolabeling with bone sialoprotein antibody revealed a positive staining for the bone nodules formed in cultures on 55S. In addition, the specific activity of ALP determined biochemically was significantly higher in 55S cultures than in the controls. SEM observations of the material surfaces after scraping off the cell layers showed that mineralized bone nodules remained attached on 55S surfaces but not on 60S. X-ray microanalysis indicated the presence of Ca and P in this bone tissue. The 55S/bone interfaces also were analyzed on transverse sections. The interfacial analysis showed a firm bone bonding to the 55S surface through an intervening apatite layer, confirmed by the X-ray mappings. All these results indicate the importance of the surface composition in supporting differentiation of osteogenic cells and the subsequent apposition of bone matrix allowing a strong bond of the bioactive materials to bone. (*J Bone Miner Res* 2001;16:231–239)

Key words: bioactive glasses, in vitro osteogenesis, mineralization, bone bonding, interfaces

¹Laboratoire de Biologie-Odontologie, Faculté de Chirurgie Dentaire, Institut Biomédical des Cordeliers, Université Paris 7, Paris, France.

²This study represents part of a dissertation to be submitted in partial fulfillment of the requirements for the degree of "Diplôme de Doctorat" by Christine Loty.

³US Biomaterials Corporation, Alachua, Florida, USA.

⁴Laboratoire de Microscopie Electronique, INSERM U314, Université de Reims, Reims, France.

⁵Laboratoire de Biologie du Développement, Université Paris 7, Paris, France.

INTRODUCTION

TISSUE ENGINEERING can be conceptualized as the use of materials to promote new tissue formation and it involves interactions of cells with the material. It has been established that the essential requirement for implantable materials to bond to living bone is the formation of a biologically active apatite layer on their surface.⁽¹⁾ For example, bioactive materials, such as calcium phosphate ceramics, bioactive glasses, and glass ceramics have been shown to form a strong chemical bond with bone. These so-called bioactive materials may influence attachment proliferation and differentiation of cells and the subsequent integration in a host tissue. Reactions occurring at the surface of bioactive glasses lead to the formation of a silica gel layer and the subsequent crystallization of hydroxycarbonated apatite (HCA).^(2,3) Hench and Ethridge⁽⁴⁾ defined key compositional features that allowed a direct bond with bone tissue: SiO₂ content must be less than 60 mol%, have high Na₂O and CaO concentrations, and have a high Ca/P₂O₅ ratio. Such compositions developed a crystalline HCA when implanted in the body that mediates a bond to both hard and soft tissues. Glasses between 53 and 56 mol% of SiO₂ formed an HCA layer at a slower rate and bond to bone but not to soft tissues. Additionally, bioactive materials are capable of releasing ions, which may affect cellular responses. For example, Matsuda and Davies⁽⁵⁾ reported in vitro a better osteoblast expression on bioactive glass than on nonreactive glass. Similarly, Vrouwenvelder et al.^(6–8) observed a stimulatory effect of 45S5 Bioglass (U.S. Biomaterials Corp., Alachua, FL, USA) on cultured rat osteoblasts in terms of cellular proliferation and differentiation. Also, these studies have provided valuable information on the effect of bioactive glasses on cell proliferation and extracellular matrix formation; they have not explored the effects of such bioactive surfaces on matrix biomineralization. Compositions similar to 55% composition used in this work have been studied for various bone grafting applications.^(9–11) Although 55S bioactive glass has been shown to bond to bone but not to soft tissue,⁽¹²⁾ the biological mechanisms concerning the interfacial reactions between the glass and the cells remain poorly understood. For this reason, this work was undertaken to examine the behavior of fetal rat osteoblasts cultured in the presence of a bioactive glass with 55 wt% silica content (55S Bioglass) and the interfacial interactions between the material and bone cells. We have used an osteoblast culture system of isolated fetal rat calvaria cells that forms nodular structures with the characteristics of woven bone.⁽¹³⁾ The aim of the present study was to investigate the supposed stimulatory effect of rat bone cells cultured in the presence of 55S Bioglass. The second objective of this work was to examine bone matrix formation and mineralization in contact with the material. Immunocytochemical and biochemical parameters showed that 55S Bioglass promoted differentiation of fetal rat osteoblasts. Furthermore, analytical scanning electron microscopy (SEM) and transmission electron microscopy (TEM) showed that the bioactive glass created a template for bone formation and allowed contact osteogenesis.

TABLE 1. BIOGLASS COMPOSITIONS (IN MOL%)

| | SiO ₂ | Na ₂ O | CaO | P ₂ O ₅ |
|-----|------------------|-------------------|------|-------------------------------|
| 55S | 55.1 | 20.1 | 22.2 | 2.6 |
| 60S | 60.1 | 17.7 | 19.6 | 2.6 |

MATERIALS AND METHODS

Materials

The materials used in this study were bioactive glasses with 55% silica and a bioinert glass composition with 60 wt% silica by weight, respectively (U.S. Biomaterials Corp., Alachua, FL, USA; Table 1). Both disks and granules were used. Disks were 20 mm in diameter and 2 mm in thickness. The size of the granules used in this study was 710–790 μm. Before exposing the bioactive glasses to cell cultures, all samples were cleaned ultrasonically in acetone and sterilized by dry heat at 180°C for 2 h in a furnace. Glasses with 60% silica by weight were used as control.

Cell culture method

Osteoblasts were isolated enzymatically from the calvaria of 21-day-old fetal Sprague–Dawley rats, as previously described by Nefussi et al.⁽¹³⁾ Briefly, calvaria were aseptically dissected and fragments were incubated in phosphate-buffered saline solution (PBS) with 0.25% collagenase (type I; Sigma, St. Louis, MO, USA) for 2 h at 37°C. Then the cells, dissociated from the bone fragments, were plated at 4 × 10⁴ cells/cm² either directly onto 55S and 60S disks or in culture dishes in the presence of loosely distributed granules (size, 710–90 μm) at a concentration of 1 mg/ml of culture medium. The culture medium used is Dulbecco's modified Eagle's medium (DMEM; Gibco, Grand Island, NY, USA) supplemented with 10% fetal calf serum (FCS; Biosis, Philadelphia, PA, USA), 10 mM β-glycerophosphate (Sigma), 50 μg/ml of ascorbic acid, and 50 U/ml of penicillin-streptomycin (Gibco). Cells were cultured up to 23 days in a humidified atmosphere of 5% in air at 37°C. Culture media were changed 24 h after seeding and at 48-h intervals thereafter.

TEM

On day 15, cultures in the presence of Bioglass particles were fixed in situ in Karnovsky solution (4% paraformaldehyde and 1% glutaraldehyde) for 1 h and rinsed in 0.2 M sodium cacodylate buffer (pH, 7.4). Bone cell cultures were then postfixated in 1% osmium tetroxide diluted in 0.2 M cacodylate buffer. Cells were then dehydrated in a graded series of alcohol, embedded in Epon-Araldite, and incubated for 1 day at 60°C. Semithin sections were cut through cell layer and biomaterial granules with a diamond knife, mounted on glass slides, and stained with toluidine blue. Semithin sections were performed for orientation purpose and then ultrathin sections were collected on copper grids and stained with 2.5% uranyl acetate in absolute ethanol for 4 minutes and lead citrate for 2 minutes. All sections were

examined using a Philips CM-12 transmission electron microscope.

SEM

Cell cultures on 55S and 60S disks were fixed on day 1 and day 10 of culture in Karnovsky fixative solution (4% paraformaldehyde and 1% glutaraldehyde) for 1 h and rinsed three times with 0.2 M sodium cacodylate buffer (pH, 7.4). Then, samples were postfixated with 1% osmium tetroxide and dehydrated in a graded series of alcohol and in amyl-acetate before critical point drying. Specimens were mounted on copper stubs with silver paints, coated with 30-nm gold in a Polaron sputtering apparatus (Kilm Fern, Milton Kayes, UK), and examined on a Jeol JSM-35 scanning electron microscope (Jeol France, Croisysurfeine, France) at 15 kV.

Cytoenzymatic localization of alkaline phosphatase

Cultured cells were fixed in situ on day 10 at room temperature in 2% citrate water solution for 30 s and dried. The cells were then exposed for 5 minutes to a solution containing naphthol AS-MX phosphate as substrate and fast violet B salt as coupler (Sigma). The cultures were incubated and observed without counterstaining. As a control, cultures were incubated in the absence of the substrate.

Immunocytochemistry

Cells cultured on Bioglass disks were fixed on day 10 with 4% paraformaldehyde for 15 minutes and cell membranes were permeabilized with 0.1% triton X-100 in PBS. After three washes of PBS, rabbit anti-rat immunoglobulin G (IgG) bone sialoprotein (dilution, 1/50; a gift from Dr L.W. Fisher, National Institute for Dental Research, National Institutes of Health [NIH], Bethesda, MD, USA) was applied for 1 h at 37°C. Subsequently, cultures were rinsed three times with PBS, incubated for 30 minutes with the second antibody, fluorescein isothiocyanate (FITC)-labeled goat anti-rabbit IgG (dilution, 1/40; Southern Biotechnology Associated, Inc., Birmingham, AL, USA). Primary antibodies were omitted in negative controls. After washes in PBS, the bioactive glass disks and control coverslips were mounted with glycerol and observed under an epifluorescence microscope (Leitz Orthoplan, Wetzlar, Germany). Photomicrographs were taken on TMAX 400 ASA film (Eastman Kodak Corp., Rochester, NY, USA).

Protein synthesis and alkaline phosphatase-specific activity assay

Before biochemical assay, osteoblastic cultures on the two substrata were prepared at different times (4 h, days 3, 5, 8, 12, 17, and 22), washed with DMEM (0% FCS) on ice, and incubated with sodium-carbonate-bicarbonate buffer (0.1 M NaHCO_3 - Na_2CO_3 , pH 10.2). Samples were stored at -80°C . For all assays (in triplicate), bone cell cultures were unfrozen and incubated in an extraction buffer (0.1 M sodium carbonate bicarbonate, pH 10.2, 1 M MgCl_2 , and 0.2% NP-40) for 10 minutes and removed of their substrate

with a rubber policeman. Cell extracts were sonicated before enzyme assay to dissociate extracellular matrix and liberate membranous alkaline phosphatase (ALP).

Estimation of protein content was carried out using the Pierce BCA Protein Assay Kit (Pierce Chemicals, Rockford, IL, USA). The specific activity of ALP was assayed in the cell layers as the release of *p*-nitrophenol from *p*-nitrophenolphosphate. The optical density was read at 410 nm in a spectrophotometer (Beckman 25; Beckman Coulter, Fullerton, CA, USA) and the enzyme activity was expressed as units per milligram of total proteins.

Energy dispersive X-ray analysis

Bone cell cultures with Bioglass particles: After 15 days in culture, samples were embedded in Epon 812. Ultrathin sections were made, collected on copper grids, and stained with 2.5% uranyl acetate in absolute ethanol for 4 minutes and lead citrate for 2 minutes. Specimens were coated with a conductive layer of carbon ($\cong 10$ nm) in a sputter coater. Sections were observed with a TEM (Philips CM 30) operating at a voltage of 50–300 kV. Energy dispersive X-ray (EDX) measurements were performed with an EDAX analyzer (SiLi detector; Oxford Instruments, Oxford, UK). EDX spectra are collected on elements with X-ray energy under 6 kV. Electron diffraction analysis was performed in micro-micro diffraction mode.

Bone cell cultures on bioactive glass disks: The extraction buffer (0.1 M sodium carbonate bicarbonate, 1 M MgCl_2 , and 0.2% NP-40) used for ALP activity assay completely removed rat bone cells with their organic matrix, and the resulting disks were prepared for SEM examinations. Each disk was washed ultrasonically in acetone and then in 70% alcohol, rinsed with distilled water, and dried before observation. A number of disks also were embedded in methyl methacrylate resin (Technovit 7200; Kulzer, Francheville, France), sectioned with a diamond saw (EXAKT; Microm, Francheville, France) to examine the bone/material interface. Specimens were mounted on copper stubs with silver paints and coated with carbon. Observations were performed with a scanning electron microscope (JSM-840A) connected to an EDX microanalyzer (EDX II; Link Analytical, Oxford Instruments).

RESULTS

Cultures with 55S Bioglass granules

Bone nodule formation: Use of phase contrast microscopy allowed for in vitro analysis of the morphological changes associated with formation of bone nodules on Bioglass granules. During the first days in culture, the cells proliferated and reached confluence by day 4 of culture. Thereafter, multilayers of cells were visible around the glass granules and formed a refringent collar that made observations of the cell outline impossible (Fig. 1A). On day 7, a differentiated area was noted at the vicinity of the glass and a refringent material could be observed in the center of this area in contact with the granule (Fig. 1B). On day 12 of culture, a change was noted by the observation that the refringent material became more opaque (Fig. 1C). Further-

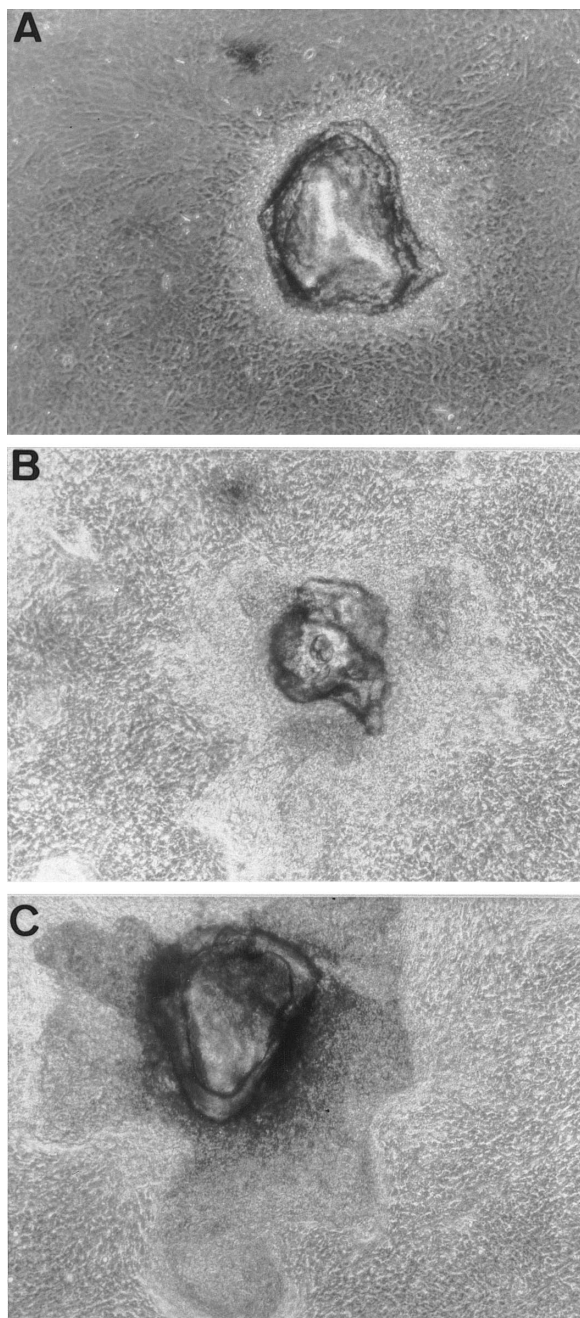


FIG. 1. Observations in phase contrast microscopy of rat bone cell culture with 55S bioactive glass particles at different times of culture. (A) Day 4 in culture. Rat bone cells proliferated and were in confluence around a 55S granule (magnification $\times 200$). (B) Day 7 in culture. A 55S bioactive particle was surrounded by differentiated areas composed of multilayers of cells with a refringent matrix (magnification $\times 200$). (C) Day 12 in culture. Bone nodules completely surrounded 55S Bioglass (magnification $\times 200$).

more, the bone nodule outline became well defined, clearly distinguishing this region from the background cell layer. The time sequence of the morphological changes noted in the 55S composition were similar to those observed with the bioinert 60S Glass (data not shown).

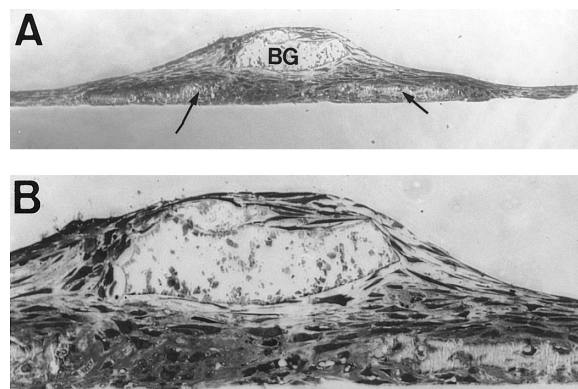


FIG. 2. (A) Semithin section of rat bone cell cultures on day 15 with 55S bioactive glass particles (magnification $\times 100$). Two bone nodules are located under the 55S particle (BG, bioactive glass; arrows, bone nodules). (B) The same semithin section at a higher magnification showing the overall morphology of bone nodules and their relationships with the 55S particle (magnification $\times 200$).

Histology: Thin sections processed perpendicularly to the cell layer (fixed on day 15) of 55S granules show bone nodules directly in contact to the material (Fig. 2A). Cross-sections through the dense glass matrix produced a breakdown of the material, which looked like a hollow zone. At a higher magnification, these bone nodules appeared to be formed of multilayered polygonal cells surrounding a mineralized zone (Fig. 2B).

TEM observation of undecalcified sections revealed the presence of a dense extracellular matrix in contact with the material (Fig. 3A). The matrix was composed of densely packed collagen fibers either cut in cross-sections or in longitudinal sections with their characteristic banding pattern. An electron-dense layer is located at the periphery of the 55S Bioglass. This layer was composed of two zones: the inner portion was granular in appearance whereas the external part is composed of needle-shaped crystals. Furthermore, collagen fibers were in close contact with the external portion of the glass, which seemed to act as a nucleating surface for biological crystals. In addition, mineralized foci were visible in the osteoid matrix that developed independently of the material and were composed of needle-shaped crystals similar to that observed at the surface of the glass. Transmission electron microscopy (TEM) observations revealed an electron-dense layer, composed of needle-shaped crystals at the periphery of the material. EDX spectrum on this electron-dense layer shows the presence of P, Pb, U, Ca, and Cu elements. Cu is caused by the copper grid. Lead and uranium are a consequence of lead citrate and uranyl acetate coloration. X-ray microanalysis revealed an accumulation of Ca and P but no Si (Fig. 3C), contrary to the inner portion (Fig. 3B), which is amorphous (Fig. 3D). The electron diffraction patterns obtained on electron-dense needle-shaped areas revealed a crystalline form (Fig. 3E).

Cultures on 55S and 60S glass disks

Osteoblast differentiation and bone nodule formation: SEM observations 24 h after seeding show that osteoblasts

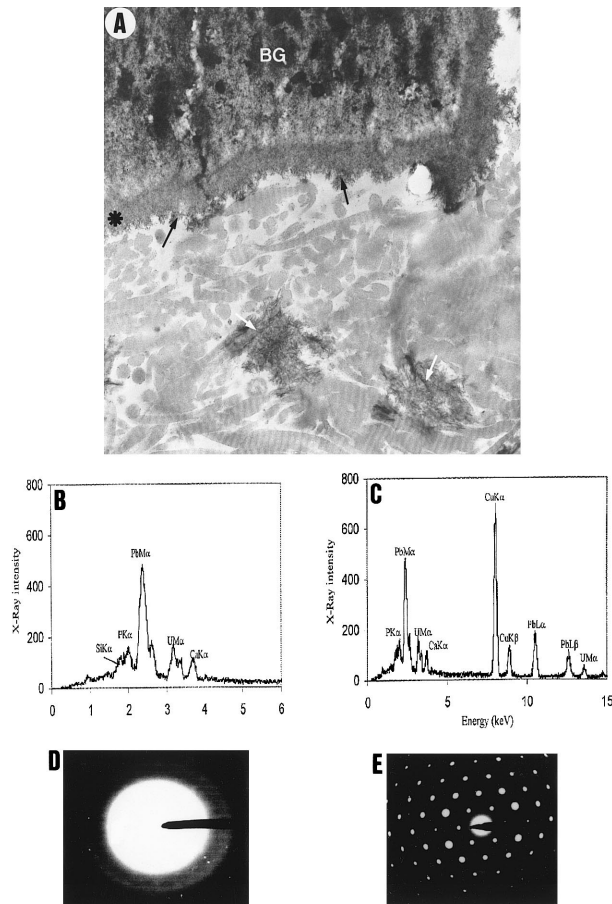


FIG. 3. (A) TEM observation of ultrathin sections of the bone cell culture with 55S granules on day 15 (BG, bioactive glass; magnification $\times 20,000$). A dense collagenous matrix is present at the periphery of the material and biological mineralized foci are visible inside the matrix (white arrows). An electron-dense layer composed of two zones surrounds the material. The interior of this electron-dense layer is granular (asterisk) whereas the external part is composed of needle-shaped crystals (black arrow). (B) EDX microanalysis of the inner part of the electron-dense layer located at the periphery of the material. X-ray spectrum reveals the presence of Si, P, and Ca. (C) EDX microanalysis of the outer part of the electron-dense layer located at the periphery of the material. X-ray spectrum reveals the presence of P and Ca but no Si. (D) Electronic diffraction pattern of the inner layer at the periphery of the material indicated that this part is poorly crystalline. (E) Electronic diffraction pattern of the outer layer at the periphery of the material indicated that this external part is crystalline.

were anchored to the 55S bioactive glass disk by means of numerous filopodia (Fig. 4A). SEM observations of rat calvaria cell cultures at day 10 showed that rat bone cells had proliferated and formed multilayered nodular structures spread into a confluent cell layer on the 55S surface (Fig. 4B).

Cytoenzymatic localization showed concentration of ALP in the bone nodules that appear as a dark region (Fig. 5). Furthermore, immunolabeling with bone sialoprotein antibody revealed a specific staining for the bone nodules in 55S cultures (Figs. 6A and 6B). It is noteworthy that osteoblast differentiation also occurred in 60S cultures and that bone nodules developed (data not shown).

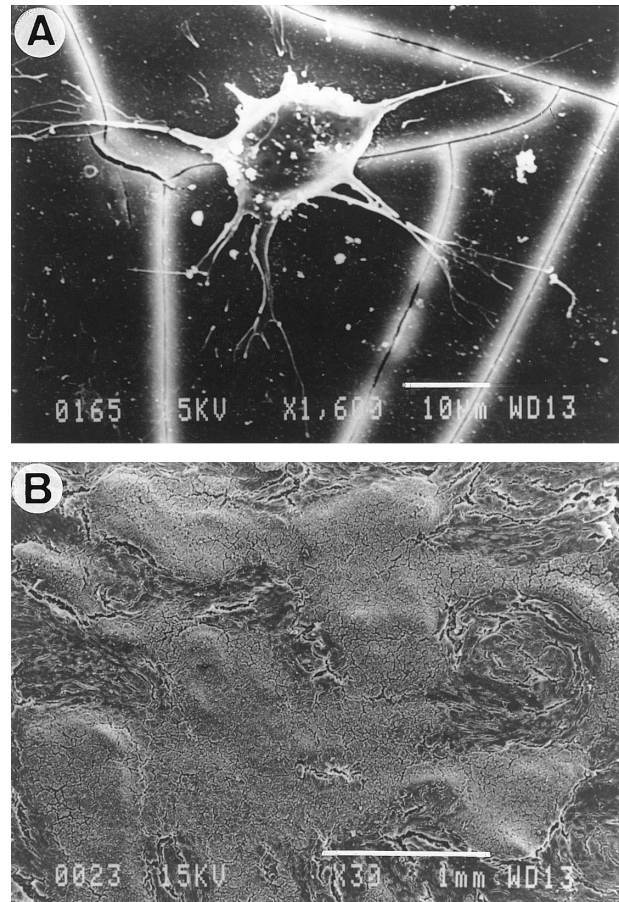


FIG. 4. (A) SEM observation of a single rat bone cell attached to the surface of a 55S disk, 24 h after seeding (bar = 10 μm). This cell anchored to the material by the means of numerous lamellipodia and exhibited a standoff morphology. (B) SEM image of the cell layer at day 10 of culture on 55S disk. Note the presence of nodular structures composed of multilayered polygonal cells (bar = 1 mm).

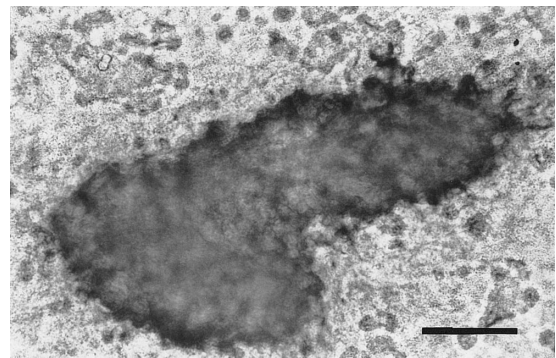


FIG. 5. Cytoenzymatic localization of ALP activity is positive in bone nodule on day 10 of culture (bar = 100 μm).

ALP activity measured by enzyme assay gradually increased after 3 days of cultures (Fig. 7). By day 8 in culture, a difference in ALP activity is seen between 55S and 60S compositions, and by day 12 this difference is 50% greater for the 55S composition.

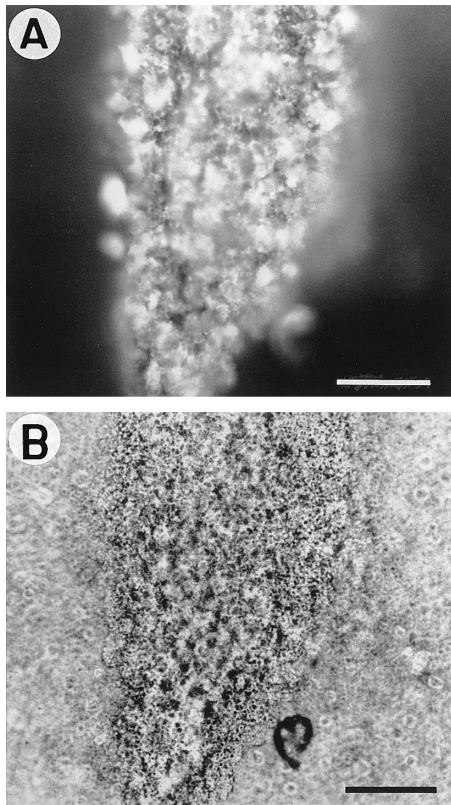


FIG. 6. (A) Immunolocalization of bone sialoprotein in culture on 55S bioactive glass showed a specific staining in the bone nodule on day 10 of culture (bar = 100 μ m). (B) The same bone nodule observed in phase contrast microscopy (bar = 100 μ m).

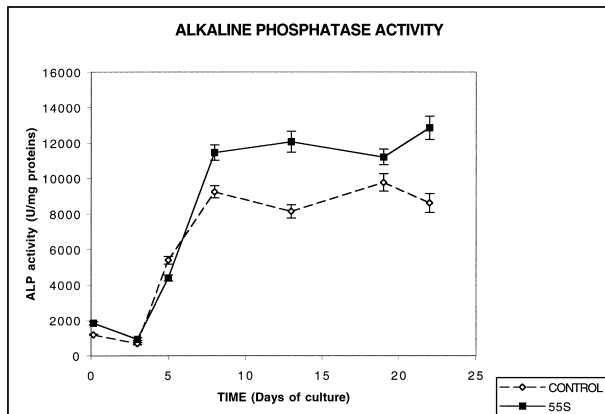


FIG. 7. Time course of ALP-specific activity during 22 days of culture on 55S disks and 60S glass control disks.

Bone bonding: The extraction buffer used for enzyme assay completely eliminated the cells and the organic matrix from the disks, and the resulting surfaces were observed under an SEM. Examination of disks after 22 days of culture revealed the presence of mineralized nodular structures attached to the surface of 55S disks (Fig. 8) but not on 60S (data not shown). Low-magnification SEM micrographs of

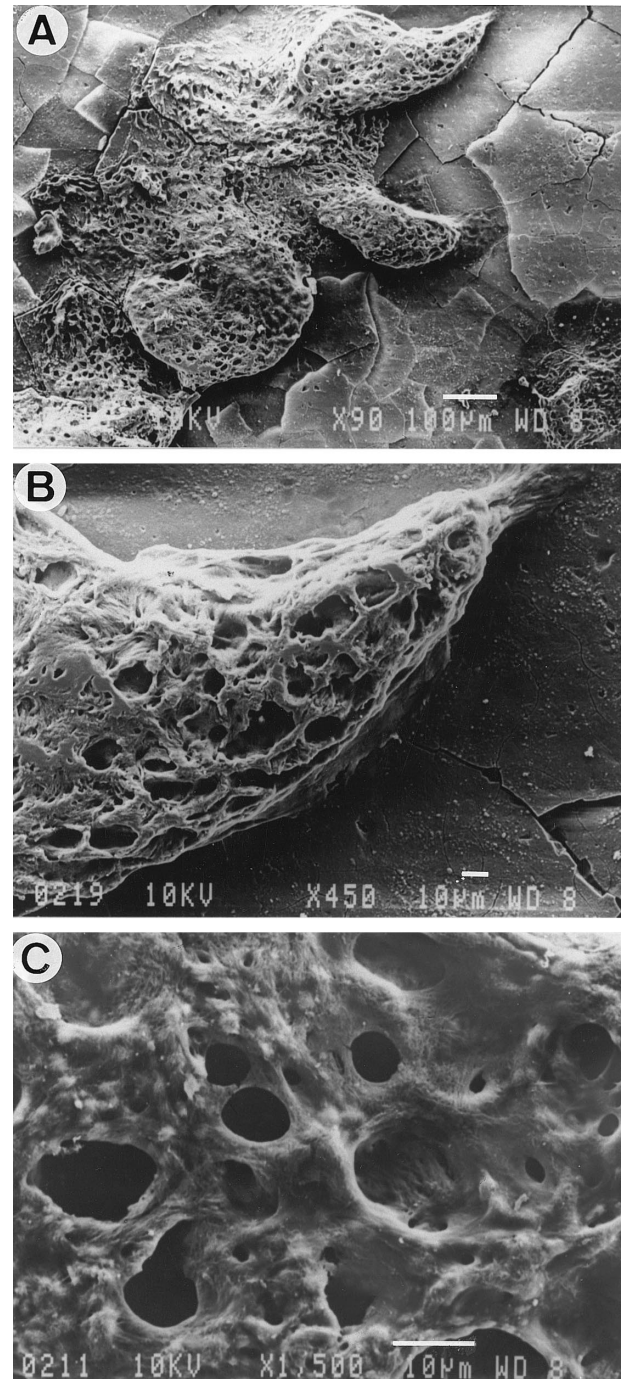


FIG. 8. SEM observations of 55S disks after elimination of the cell layer and the organic matrix, after 22 days of culture. (A) SEM examination revealed the presence of irregular nodular structures that remained attached to the 55S surface (magnification $\times 90$). (B) At a higher magnification, this bone nodule appeared as a spongy structure with numerous osteocytes lacunae (magnification $\times 450$). (C) The same nodule at a higher magnification (magnification $\times 1500$).

the disks showed evidence of the presence of mineralized bone nodules in contact with the bioactive glass (Fig. 8A). Furthermore, the surface of the glass is covered with the reactive surface and exhibited cracks due to the SEM prep-

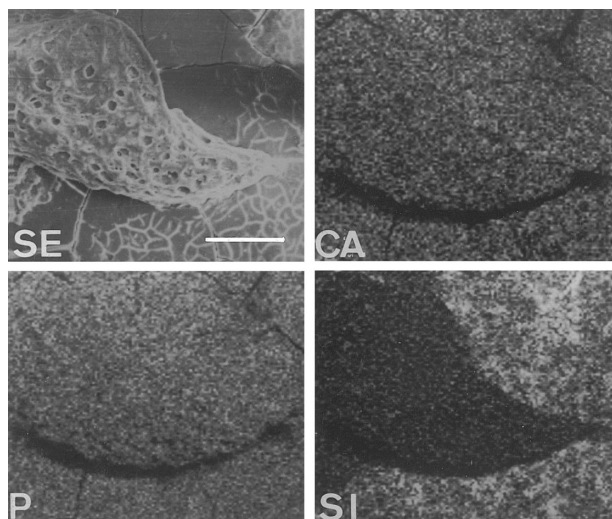


FIG. 9. EDX mapping of bone nodule observed in Fig. 8 by SEM with secondary electrons (SE) showed the presence of P and Ca in the nodule but no Si (bar = 100 μm).

arations. At a higher magnification, a mineralized bone nodule attached to 55S appeared as a spongy structure with numerous lacunae, corresponding to osteocyte cell processes that were very similar to trabecular bone (Figs. 8B and 8C). EDX mapping of the surface of 55S indicated the presence of Ca and P (Fig. 9) with a little silicon (Table 2). The mineralized bone nodule contained calcium and phosphorus (Fig. 9) with a Ca/P ratio similar to the glass surface layer, but no silicon (Table 2).

The SEM (secondary and backscattered electrons) and X-ray microanalysis of the sectioned disks examined the interface between the mineralized bone matrix and bioactive glass. Figure 10A shows a section of a 55S disk on which rat osteoblasts have been cultured 22 days and where the cells have been removed as explained previously. The SEM micrograph shows continuity between the ceramic and a bonelike structure that seems to be mediated by an intermediate layer. These findings were confirmed using backscattered electron microscopy where the mineralized bone nodule was clearly visible with osteocyte lacunae inside the mineralized matrix (Fig. 10B). X-ray microanalytical mappings of the bone mineralized nodule/55S Bioglass interface indicated the distribution of Ca and P throughout the material and the bone tissue (Fig. 10C). Si was present in the glass bulk but in larger amounts beneath the Ca-P-rich layer.

DISCUSSION

Osteoblast differentiation

Bioactive materials have been defined based on a specific biological response elicited when implanted into bone. This concept is based on control of the surface chemistry of the material. Reactions occurring at the surface of bioactive glasses lead to the formation of a silica gel layer and the subsequent crystallization of HCA.^(2,3) The results of the present study showed that a bioactive glass with 55 wt%

silica content 55S Bioglass promoted differentiation of fetal rat osteoblasts. Furthermore, the glass created a template for bone formation and allowed contact osteogenesis.

Immunocytochemical and biochemical data clearly indicated a positive effect of 55S Bioglass on osteogenic differentiation. Our findings agree with those of Vrouwenvelder et al.⁽⁶⁻⁸⁾ who observed a stimulatory effect of 45S5 Bioglass on cultured rat osteoblasts. In the same way, Matsuda and Davies⁽⁵⁾ showed a better cellular colonization and extracellular matrix production on bioactive glasses versus nonbioactive glasses in calvaria organ cultures. Cells are sensitive to the physicochemical characteristics of the materials with which they interact. This is the case particularly for bioactive glasses that release ions and create on their surface a microenvironment that could positively influence the behavior of the cells. The reaction kinetics of bioactive glasses has been studied extensively after incubation in simulated body fluids. Glasses with a higher level of bioactivity undergo surface reactions very rapidly, for example, within 3 h for 45S5 Bioglass, and lead to the formation of an HCA layer on its surface.^(14,15) The more gradual development of a crystalline HCA on 55S Bioglass results in interactions of the cells with the reactive interface over a longer period of time. Furthermore, the ion exchange created an alkaline pH at the surface of the Bioglass that could encourage osteoblast differentiation.

This phenomenon of ion exchange that also occurred in the culture medium could explain the promotion of the osteoblast phenotype in 55S Bioglass cultures. A recent study provides evidence that this hypothesis is valid. This study showed that soluble extracts of bioactive glasses enhanced bone mineralization in organ cultures.⁽¹⁶⁾ Likewise, it was shown that the process of bone formation depended on an optimal alkaline pH in the extracellular milieu surrounding the osteoblasts.⁽¹⁷⁾ On the other hand, others have shown that the products of glass corrosion elevated the pH of the culture medium to a value that adversely affects osteoblast activity. To prevent pH shifts, these authors immersed the material in Tris buffer before the cultures.^(18,19) This discrepancy may be related to differences in the composition of the glasses and their surface reaction kinetics.

A biological explanation of the stimulatory effect of an alkaline pH on osteoblast differentiation concerned the regulation of gap junction intercellular communications. Yamaguchi et al.⁽²⁰⁾ have shown that the gap junction coupling was increased at an alkaline pH in MC3T3-E1 osteoblastic cells. Gap junction communication seemed to play a key role during cellular condensations that proceeded in vivo as well as in vitro osteoblast differentiation.⁽²¹⁾ The increased pH created by the reaction of the 55S glass may be enhancing gap junction communication, thereby increasing osteoblast differentiation.

Authors have reported that 55S Bioglass releases soluble silicon immediately on exposure of the glass to an in vitro solution or to body fluids.^(4,22,23) For example, silicon was known to ensure a structural role in the formation of crosslinks between collagen and proteoglycans during bone growth.⁽²⁴⁾ A potential metabolic function served by soluble silicon was shown in an elegant work by Keeting et al.,⁽²⁵⁾ which showed that zeolite-A present in soluble silicon stim-

TABLE 2. ELEMENT ATOMIC PERCENTAGE OF THE INTERFACE BONE/55S

| | Si K | Ca K | P K | Na K | O K |
|----------------------|------|------|-----|------|------|
| Bone nodule on 55S | 0.2 | 16.2 | 8.9 | -0.0 | 74.7 |
| Apatite layer on 55S | 2.0 | 15.7 | 8.6 | -0.3 | 74.0 |
| Si-rich layer on 55S | 21.0 | 2.0 | 1.2 | 0.1 | 75.7 |
| 55S bioactive glass | 13.0 | 7.1 | 1.4 | 9.0 | 68.9 |

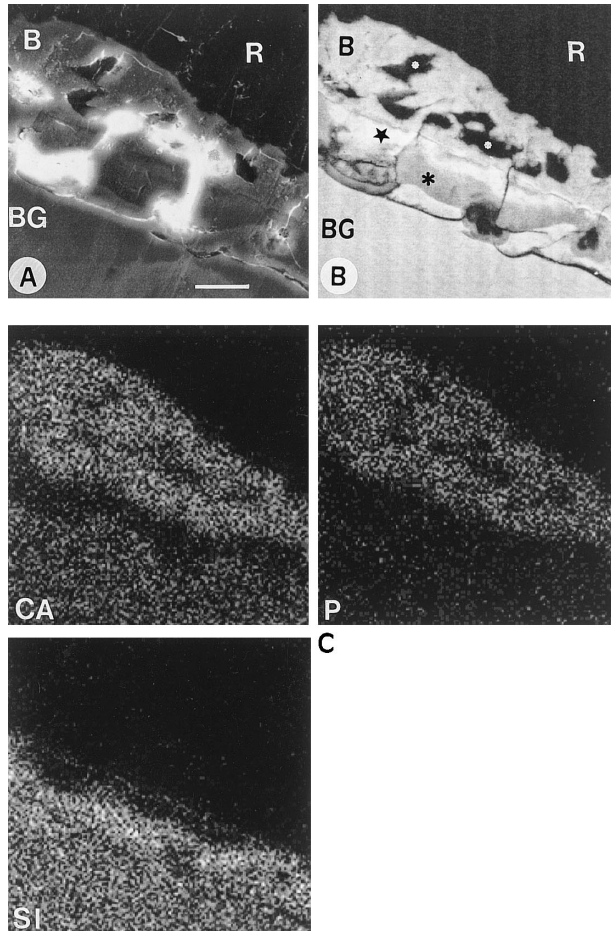


FIG. 10. SEM observations and EDX analysis of the interface between bone nodules and 55S sectioned disks after elimination of the cell layer on day 22 of culture. (A) SEM image by secondary electrons (R, resin; B, bone nodule; BG, bioactive glass; bar = 10 μm). (B) The same zone observed by backscattered electron microscopy (black star, Ca-P-rich layer; black asterisk, Si-rich layer; white asterisks, osteocyte lacunae). (C) EDX mapping of the interface. Results showed the presence of Ca and P in the bone nodule, a Ca-P-rich layer under the nodule, and a Si-rich layer under the Ca-P-rich layer.

ulated human osteoblast proliferation and differentiation by regulating transforming growth factor β (TGF- β) production. In our study, the negatively charged silica gel that formed at the surface of the bioglasses before crystallization could have adsorbed adhesion molecules and growth factors and subsequently promoted osteoblast differentiation. Finally, we can hypothesize that the stimulatory effect of 55S Bioglass on osteoblast differentiation is caused by a dy-

namic surface chemistry that provides an extracellular stimulus to the cell and an extracellular environment that is compatible with adsorption of biologically active molecules.

Matrix mineralization and contact osteogenesis

Another important finding reported in this study confirms in vitro the capacity of mineralized bone tissue to form directly on 55S bioactive glass and to bond with it. Bioactive implants have differing rates of bonding depending on their bulk composition. For example, glass compositions with more than 60% SiO_2 do not bond to bone. The present study confirmed this data and showed evidence of bone apposition to the surface of the bioactive glass but not on the 60S bioinert surface. This finding is surprising because osteoblast differentiation and bone nodule formation occurred normally on 60S glass. Hence, the bioactive surface not only encouraged osteoblast differentiation but also allowed contact osteogenesis. In contrast, mineralized bone nodules were not present on the 60S surface after crapping-off the cell layers. It is possible that bone nodules formed on 60S developed at a distance from the glass surface, inside the multicellular layers. Another explanation is that the mineralized bone nodules were in contact (but not bond) with the bioinert surface and have been removed by the mechanical action of the rubber policeman and the ultrasonic cleaning of the disks. This probably is because of the fact that the bioinert 60S surface does not develop a well HCA layer to which cells can attach. SEM observations of mineralized bone nodules at the bone/55S Bioglass interface, and analysis of calcium, phosphorus, and silicon evidenced the ability of the bioactive glass to bond with bone. Bioactive glasses formed a hydrated silica-gel layer within minutes of exposure to body fluids.⁽²²⁾ In addition, soluble silicon accelerated the precipitation of an amorphous calcium phosphate, and silanol, soluble organic silicon, provided a heterogeneous mechanism for hydroxyl carbonate apatite.⁽²⁶⁾ In our study, the bioactive surface was confirmed to be composed of calcium and phosphorous and was highly crystallized. Furthermore, collagen fibrils coalesced with this layer, which seemed to act as a nucleating surface for biological crystals. Such observations suggested that at early stages of osteogenesis, calcified foci might serve to bridge to collagen fibers and thereby create a continuous mineralized bone tissue and allow fusion with the surface layer of the glass. Hench and Paschall⁽¹⁾ first reported the bonding of bioactive glasses by interdigitation of collagen fibers with the material surface. Last, we have previously shown in a TEM study that AW glass-ceramic bonded to bone formed in vitro through the formation of a Ca-P-rich

layer.⁽²⁷⁾ Furthermore, we showed that biomineralization can be initiated on the bioactive layer, which acts as a nucleating surface for biological crystals and then serves as a template for the organization of the matrix. Richard et al.⁽²⁸⁾ showed, by TEM and electron diffraction, that calcium phosphate implants encourage an epitaxial biological crystal deposition, which supports the data of the present investigation.

In conclusion, there appears to be a better osteoblast expression on 55S bioactive glass compared with bioinert 60S glass as shown by enzyme cytochemical, immunocytochemical, and biochemical parameters. Furthermore, mineralization can be initiated in vitro with 55S bioactive glass serving as a nucleating surface and a template for the organization of the matrix and for generating bone tissue.

ACKNOWLEDGMENTS

The authors are grateful for SEM investigations performed by the "Center Inter-Universitaire de Microscopie Electronique" Jussieu, Universités Paris VI et Paris VII, CNRS, 7, quai Saint Bernard, 75252 Paris Cedex 05, France. We thank F. Meury for expert technical assistance. This work was supported by a grant from CANAM—Assistance Publique—Hôpitaux de Paris and by INSERM and CNRS (n°4M109D). This work also was supported by the U.S. Biomaterials Corp., Alachua, FL, USA.

REFERENCES

- Hench LL, Paschall HA 1973 Direct chemical bonding between bioactive glass-ceramic materials and bone. *J Biomed Mater Res Symp* **4**:25–42.
- Clark AE, Pantano CG, Hench LL 1976 Auger spectroscopic analysis of bioglass corrosion films. *J Am Ceram Soc* **59**:37–39.
- Ogino M, Ohuchi F, Hench LL 1980 Compositional dependence of the formation of calcium phosphate films on bioglass. *J Biomed Mater Res* **14**:55–64.
- Hench LL, Ethridge EC 1982 *Biomaterials: An interfacial approach*. Biophysics and Bioengineering Series No. 4, Academic Press, London, UK, pp. 221–254.
- Matsuda T, Davies JE 1987 The in vitro response of osteoblasts to bioactive glass. *Biomaterials* **8**:275–284.
- Vrouwenvelder WCA, Groot GC, de Groot K 1992 Behavior of fetal rat osteoblasts cultured in vitro on bioactive glass and nonreactive glass. *Biomaterials* **13**:382–392.
- Vrouwenvelder WCA, Groot GC, de Groot K 1993 Histological and biochemical evaluation of osteoblasts cultured on bioactive glass, hydroxyapatite, titanium alloy, and stainless steel. *J Biomed Mater Res* **27**:465–475.
- Vrouwenvelder WCA, Groot GC, de Groot K 1994 Better histology and biochemistry for osteoblasts cultured on titanium-doped bioactive glass: 45S5 compared with iron, titanium, fluoride and boron-containing bioactive glasses. *Biomaterials* **15**:7–106.
- Larmas E, Sewon L, Loustarinen T, Kangasniemi I, Yli-Urpo A 1995 Bioactive glass in periodontal defects. Initial findings of soft tissue and osseous repair. In: Wilson J, Hench LL, Greenspan G (eds.) *Bioceramics*, vol. 8. Elsevier Science, Oxford, UK, pp. 279–284.
- Suominen E, Kinnunen J 1996 Bioactive glass granules and plates in the reconstruction of defects of facial bones. *Scand J Plast Reconstr Surg Hand Surg* **30**:281–289.
- Aitasalo K, Sounpaa J, Peltola M, Yli-Urpo A 1997 Behavior of bioactive glass (S53P4) in human frontal sinus obliteration. In: Sedel L, Rey C (eds.) *Bioceramics*, vol. 10, Elsevier Science, Oxford, UK, pp. 429–432.
- Hench LL, Wilson J 1998 *Bioactive glasses: Present and future*. In: LeGeros RZ, LeGeros JP (eds.) *Bioceramics*, vol. 11. World Scientific, New York, NY, USA, pp. 31–36.
- Nefussi JR, Boy-Lefevre ML, Boulekbache H, Forest N 1985 Mineralization in vitro of matrix formed by osteoblasts isolated by collagenase digestion. *Differentiation* **29**:60–168.
- Clark AE, Pantano CG, Hench LL 1976 Auger spectroscopic analysis of bioglass corrosion films. *J Am Ceram Soc* **59**:37–39.
- Kim CY, Clark AE, Hench LL 1988 Early stages of calcium-phosphate layer formation on bioglasses. *J Non Crystalline Solids* **113**:195–202.
- Maroothernaden J, Zang X, Hench LL, Revell PA 1998 Effect of bioglass and loading environment on whole bone organs cultured in vitro. In: LeGeros RZ, LeGeros JP (eds.) *Bioceramics*, vol. 11. World Scientific, New York, NY, USA, pp. 501–504.
- Green J 1994 Cytosolic pH regulation in osteoblasts. *Miner Electrolyte Metab* **20**:16–30.
- El Ghannam A, Ducheyne P, Shapiro IM 1995 Bioactive material template for in vitro synthesis of bone. *J Biomed Mater Res* **29**:359–370.
- El Ghannam A, Ducheyne P, Shapiro IM 1997 Formation of surface reaction products on bioactive glass and their effects on the expression of the osteoblastic phenotype and the deposition of mineralized extracellular matrix. *Biomaterials* **18**:295–303.
- Yamaguchi DT, Huang JT, Ma D 1995 Regulation of gap junction intercellular communication by pH in MC3T3-E1 osteoblastic cells. *J Bone Miner Res* **10**:1891–1899.
- Hall BK, Miyake T 1995 Divide, accumulate, differentiate: Cell condensation in skeletal development revisited. *Int J Dev Biol* **39**:881–893.
- Ogino M, Ohuchi F, Hench LL 1980 Compositional dependence of the formation of calcium phosphate films on bioglass. *J Biomed Mater Res* **14**:55–64.
- Hench LL, Wilson J 1984 Surface-active biomaterials. *Science* **226**:630–636.
- Hott M, de Pollak C, Modrowski D, Marie PJ 1993 Short-term effects of organic silicon on trabecular bone in mature ovariectomized rats. *Calcif Tissue Int* **53**:174–179.
- Keeting PE, Oursler MJ, Wiegand KE, Bonde SK, Spelsberg TC, Riggs BL 1992 Zeolite A increases proliferation, differentiation and transforming growth factor beta production in normal adult human osteoblast-like cells in vitro. *J Bone Miner Res* **7**:1281–1289.
- Damen JJ, ten Cate JM 1989 The effect of silicic acid on calcium phosphate precipitation. *J Dent Res* **68**:1355–1359.
- Sautier JM, Kokubo T, Ohtsuki T, Nefussi JR, Boulekbache H, Oboeuf M, Loty S, Loty C, Forest N 1994 Bioactive glass-ceramic containing crystalline apatite and wollastonite initiates biomineralization in bone cell culture. *Calcif Tissue Int* **55**:458–466.
- Richard M, Aguado E, Cottrel M, Daculsi G 1998 Ultrastructural and electron diffraction of the bone-ceramic interfacial zone in coral and biphasic CaP implants. *Calcif Tissue Int* **62**:437–442.

Address reprint requests to:

Dr. Christine Loty
Laboratoire de Biologie-Odontologie
Institut Biomédical des Cordeliers
15–21, rue de l'École de Médecine
F-75270 Paris Cedex 06, France

Received in original form December 3, 1999; in revised form May 25, 2000; accepted July 18, 2000.